

Time Reversal Communication in Rayleigh-Fading Broadcast Channels with Pinholes

Albert C. Fannjiang

^a *Department of Mathematics, University of California, Davis 95616-8633*

Abstract

The paper presents an analysis of the time reversal in independent-multipath Rayleigh-fading channels with N inputs (transmitters) and M outputs (receivers). The main issues addressed are the condition of statistical stability, the rate of information transfer and the effect of pinholes. The stability condition is proved to be $MC \ll N_{\text{eff}}B$ for broadband channels and $M \ll N_{\text{eff}}$ for narrowband channels where C is the symbol rate, B is the bandwidth and N_{eff} is the *effective* number (maybe less than 1) of transmitters. It is shown that when the number of screens, $n - 1$, is relatively low compared to the logarithm of numbers of pinholes N_{eff} is given by the *harmonic* (or *inverse*) *sum* of the number of transmitters and the numbers of pinholes at all screens. The novel idea of the effective number of time reversal array (TRA) elements is introduced to derive the stability condition and estimate the channel capacity in the presence of multi-screen pinholes. The information rate, under the constraints of the noise power ν per unit frequency and the average total power P , attains the supremum P/ν in the regime $M \wedge N_{\text{eff}} \gg P/(\nu B)$. In particular, when $N_{\text{eff}} \gg M \gg P/(B\nu)$ the optimal information rate can be achieved with statistically stable, sharply focused signals.

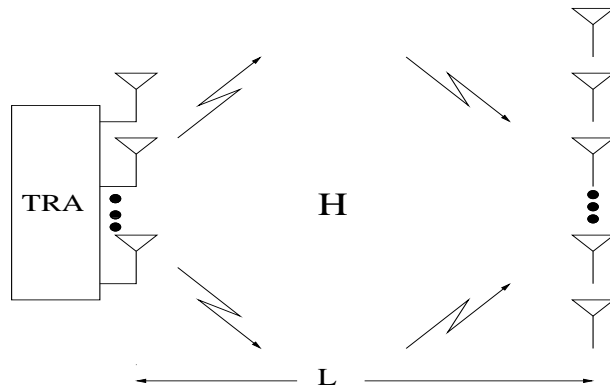


Fig. 1. MIMO Broadcast Channel

1 Introduction

Time reversal (TR) of waves has received great attention in recent years and been extensively studied for electromagnetic [2], [20] as well as acoustic propagation (see [14] and the references therein). A striking effect of time reversal in randomly inhomogeneous media is the superresolution of refocal signals [1], [13] which implies low probability of intercept and holds high potential in technological applications such as communications [9], [25], [10], [17],[18].

An issue prior to superresolution, however, is statistical stability, namely the question: How many antennas and how much bandwidth does one need to achieve self-averaging in TR so that the received signals are nearly deterministic, independent of the channel statistics? In this paper we answer this question for independent-multipath Rayleigh fading channels, with multiple inputs and multiple outputs (MIMO), commonly used in wireless communication literature, see, e.g. [23]. We also introduce the novel idea of effective number of transmitters to analyze the effect of multi-screen pinholes on stability and capacity.

In the MIMO-TR communication scheme as studied in [9], [12], the M well-separated receivers first send a pilot signal to the N -element time reversal array (TRA) which then uses the time-reversed version of the received signals to modulate the data symbols and retransmit them back to the receivers. One of the main results obtained here is that the time reversal process is statistically stable when

Email address: cafannjiang@ucdavis.edu (Albert C. Fannjiang).

URL: <http://www.math.ucdavis.edu/~fannjian> (Albert C. Fannjiang).

¹ I thank the American Institute of Mathematics and the organizers of the Workshop “Time-Reversal Communications in Richly Scattering Environments”, October 18-22, 2004, for a stimulating meeting which motivated the present work. This research is partially supported by U.S. National Science Foundation grant DMS 0306659.

$$MC \ll N_{\text{eff}}B, \quad \text{for broadband channels} \quad (1)$$

$$M \ll N_{\text{eff}}, \quad \text{for narrowband channels} \quad (2)$$

where $C(\leq 2B)$ is the symbol rate, B is the bandwidth and N_{eff} is the *effective* number of transmitters (maybe less than one). In the presence of $(n-1)$ -screen pinholes, we show that the effective number of transmitters is asymptotically the harmonic sum of the number of transmitters and the number of pinholes of every screen when all these numbers are greater than 2^n .

The LHS of (1) is the number of degrees of freedom per unit time in the constellation of input data-streams while the RHS of (1) is roughly the number of degrees of freedom per unit time in the channel state information (CSI) received by TRA from the pilot signals. The latter has to be larger than the former in order to reverse the random scrambling by the channel and achieve deterministic outputs. The stability condition $N \gg 1$ for narrowband channels or $B \gg \beta_c$ (the coherence bandwidth) for broadband channels, when M is small and the pinholes are absent, have been previously discussed in [1], [7], [8], [9], [20].

In Section 4 and 5.2, we analyze the information rate of the TR broadcast channel in the presence of noise. We show that the optimal information rate $R \sim P/\nu$, under the power and noise constraints, can be achieved in the regime $M \wedge N_{\text{eff}} \gg P/(\nu B)$ where ν is the magnitude of noise per unit frequency and P the average total power input. In particular, when $N_{\text{eff}} \gg M \gg P/(B\nu)$ the optimal information rate can be achieved with statistically stable, sharply focused signals.

2 TR-MIMO communication

First let us review the MIMO-TR communication scheme as described in [12] which is an example of broadcast channel [23].

The M receivers located at $\mathbf{y}_j, j = 1, \dots, M$ first send a pilot signal $\int e^{i\omega t} g(B^{-1}(\omega - \omega_0)) d\omega \delta(\mathbf{x} - \mathbf{y}_j)$ to the N -element TRA located at $\mathbf{x}_i, i = 1, \dots, N$ which then uses the time-reversed version of the received signal $\int e^{i\omega t} g(B^{-1}(\omega - \omega_0)) H(\mathbf{y}_j, \mathbf{x}_i; \omega) d\omega$ to encode a stream of symbols and retransmit them back to the receivers. Here H is the transfer function of the propagation channel at the frequency ω from point \mathbf{y} to \mathbf{x} and $g^2(\omega)$ is the power density at ω . Let $\mathbf{H}(\omega) = [H_{ij}(\omega)], H_{ij}(\omega) = H(\mathbf{x}_i, \mathbf{y}_j; \omega)$, be the transfer matrix between the transmitters and receivers. The reciprocity implies that $H(\mathbf{y}_j, \mathbf{x}_i; \omega) = H_{ij}(\omega)$ and $\mathbf{H}^*(\omega) = \mathbf{H}(-\omega)$ where $*$ stands for complex conjugation. Let us assume that g is a smooth and rapidly decaying function such as the Gaussian function. Naturally the relative bandwidth B/ω_0 is less than unity so that $\omega_0 \gg 1$

if $B \gg 1$. In this paper we will assume $B/\omega_0 \ll 1$ to simplify the frequency coherence structure below (Section 3). We have chosen the time unit such that the speed of propagation is one and the wavenumber equals the frequency.

The signal vector $\mathbf{S} = (S_j)$ arriving at the receivers with delay $L + t$ is then given by [12] (see also [1], [6])

$$S_j(t) = \sum_{l=1}^W \sum_{i=1}^M m_i(\tau_l) \int e^{-i\omega(t-\tau_l)} g\left(\frac{\omega - \omega_0}{B}\right) \sum_{k=1}^N H_{jk}(\omega) H_{ik}^*(\omega) d\omega \quad (3)$$

where $m_j(\tau_l), l = 1, \dots, W \leq \infty$ is a stream of symbols intended for the j -th receiver transmitted at times $\tau_l = l\tau, \tau > 0$. In vector notation, we have $\mathbf{S} = \sum_{l=1}^W \int e^{-i\omega(t-\tau_l)} g(B^{-1}(\omega - \omega_0)) \mathbf{H} \mathbf{H}^\dagger(\omega) \mathbf{m}(\tau_l) d\omega$ where \mathbf{H}^\dagger is the conjugate transpose of \mathbf{H} and $\mathbf{m}(\tau_l) = (m_j(\tau_l))$. Let us note that while all the TRA-elements are coordinated and synchronized the receivers do not know the channel and can not coordinate in decoding the total signal vector received. As a consequence, the multi-user interference arises and can be a serious impedance to communications. An advantage of the time reversal scheme is the possibility to use the (statistical) stability property to achieve the following asymptotic

$$\int e^{-i\omega(t-\tau_l)} g\left(\frac{\omega - \omega_0}{B}\right) \sum_{k=1}^N H_{jk}(\omega) H_{ik}^*(\omega) d\omega \sim B \delta_{ij} e^{-i\omega_0(t-\tau_l)} \mathcal{F}^{-1}[g](B(\tau_l - t))$$

so that $S_j(t) \sim B \sum_{l=1}^W m_j(\tau_l) e^{-i\omega_0(t-\tau_l)} \mathcal{F}^{-1}[g](B(\tau_l - t))$ and each receiver receives the input symbols with little interference. Here and below \mathcal{F}^{-1} stands for the inverse Fourier transform.

3 Statistical stability

One of the main goals of the present note is to characterize the stability regime for the independent-multipath Rayleigh fading channel in which $H_{ij}(\omega)$ are independent $\mathcal{CN}(0, \sigma)$, the zero-mean, variance- σ circularly symmetric complex-Gaussian random variables and $\{H_{ij}(\omega)\}_{i,j,\omega}$ are a *jointly* Gaussian process. The independent-multipath Rayleigh fading is an idealized model for richly scattering environment, after proper normalization, when the spacings within the transmitters and receivers are larger than the coherence length ℓ_c of the channel. In general, the coherence length is inversely proportional to the angular spread [23] and sometimes can be computed explicitly in terms of physical properties of the channel [12]. For diffuse waves the coherence length is known to be on the scale of wavelength [28], [27].

We set the variance $\sigma = 1/(N \vee M)$ so that the average input power is no less than the average output power. The value of σ would not change the conditions of statistical stability but will affect the discussion of information transfer in the next section.

Let us calculate the mean and the variance of the signals with respect to the ensemble of the channel. Let \mathbb{E} denote the channel ensemble average. For simplicity, we assume that $|m_i(\tau_l)| = \mu, \forall i, l$. By the Gaussian rule for the calculation of moments we have

$$\mathbb{E}\mathbf{S} = BN\sigma\mathbf{m} \sum_{l=1}^W e^{-i\omega_0(t-\tau_l)} \mathcal{F}^{-1}[g](B(t-\tau_l)). \quad (4)$$

Let $\tau \geq (2B)^{-1}$ so that the summation in $\mathbb{E}\mathbf{S}$ is B -uniformly bounded as $W \rightarrow \infty$.

The statistical stability of the signals can be measured by the normalized variance of the signals at the receiver j

$$\mathcal{V}_j(\tau_n) = \frac{V_j(\tau_n)}{|\mathbb{E}S_j|^2(\tau_n)}, \quad V_j(\tau_n) \equiv \mathbb{E}|S_j|^2(\tau_n) - |\mathbb{E}S_j(\tau_n)|^2,$$

$\forall j, n$ and the time-reversed signals are stable when $\mathcal{V}_j(\tau_n) \rightarrow 0, \forall j, n$. Note that $\mathcal{V}_j^{-1}(\tau_l)$ is exactly the signal-to-interference ratio (SIR) at receiver j .

Let β_c be the coherence bandwidth of the channel such that

$$\mathbb{E}[H_{ij}(\omega)H_{i'j'}^*(\omega')] \approx \sigma f(\omega_0, \frac{\omega - \omega'}{\beta_c}) \delta_{ii'} \delta_{jj'}$$

where $f(\omega_0, \cdot)$ is a continuous, rapidly decaying function and $f(\omega_0, 0) = 1$ (see [11], [12] for a rigorous example). Here we have used the fact that the relative bandwidth B/ω_0 is small so that f is independent of the precise value of the frequency. Below we shall suppress the argument ω_0 in f . The coherence bandwidth β_c is inversely proportional to the delay spread and hence the delay-spread-bandwidth product (DSB) is roughly $B\beta_c^{-1}$ [11], [12], [23]. In the diffusion approximation β_c is given by the Thouless frequency $D_B L^{-2}$ where D_B is the Boltzmann diffusion constant, equal to the energy transport velocity times the transport mean free path, and L the distance of propagation [19], [29].

The *broadband, frequency-selective* (BBFS) channel is naturally defined as having a large DSB, i.e. $B\beta_c^{-1} \gg 1$. Since $B < \omega_0, \omega \in [\omega_0 - B/2, \omega_0 + B/2]$ and $-\omega$ are separated by more than β_c in a BBFS channel. On the other hand,

$B \ll \beta_c$ corresponds to the *narrow-band, frequency-flat* (NBFF) channel. For convenience in the subsequent analysis, we shall think of the NBFF channel as the limit $\beta_c \rightarrow \infty$ and the BBFS channel as the limit $\beta_c \rightarrow 0$ while ω_0, B are fixed. In either case, we have

$$V_j(t) \approx N\sigma^2 \sum_{i=1}^M \sum_{l,l'=1}^W m_i(\tau_l) m_i^*(\tau_{l'}) e^{i\omega_0(\tau_l - \tau_{l'})} \times \int d\omega d\omega' e^{-i(\omega - \omega')(t - \tau_l)} e^{i\omega'(\tau_l - \tau_{l'})} g\left(\frac{\omega}{B}\right) g^*\left(\frac{\omega'}{B}\right) |f|^2\left(\frac{\omega - \omega'}{\beta_c}\right). \quad (5)$$

Consider the NBFF channels first. We obtain by passing to the limit $\beta_c \rightarrow \infty$

$$V_j(t) \approx N\sigma^2 B^2 |f|^2(0) \sum_{i=1}^M \left| \sum_{l=1}^W m_i(\tau_l) e^{i\omega_0 \tau_l} \mathcal{F}^{-1}[g](B(t - \tau_l)) \right|^2.$$

In view of (4) the stability condition $N \gg M$ for NBFF channels then follows easily. On the other hand, the BBFS channels ($\beta_c \rightarrow 0$) yields

$$V_j(t) \approx N\sigma^2 \sum_{i=1}^M \sum_{l,l'=1}^W m_i(\tau_l) m_i^*(\tau_{l'}) e^{i\omega_0(\tau_l - \tau_{l'})} \times \int d\omega'' d\omega' e^{-i\omega''(t - \tau_l)} e^{i\omega'(\tau_l - \tau_{l'})} g\left(\frac{\omega'}{B}\right) g^*\left(\frac{\omega'}{B}\right) |f|^2\left(\frac{\omega''}{\beta_c}\right) \approx N\sigma^2 B\beta_c \sum_{i=1}^M \sum_{l=1}^W m_i(\tau_l) \mathcal{F}^{-1}[|f|^2](\beta_c(\tau_l - t)) \times \sum_{l'=1}^W m_i^*(\tau_{l'}) e^{i\omega_0 \tau(l-l')} \mathcal{F}^{-1}[|g|^2](B\tau(l-l')). \quad (6)$$

Several observations are in order. First, due to $\tau \geq (2B)^{-1}$ the summation over l' in (6) is convergent as $W \rightarrow \infty$ uniformly in B . Second, due to the term $\mathcal{F}^{-1}[|f|^2](\beta_c(\tau_l - t))$, there are effectively $C\beta_c^{-1}$ terms in the summation over l where $C = \tau^{-1}$ is the number of symbols per unit time in each data-stream. As a result, the variance $V_j \sim N\sigma^2 BMC\mu^2$ is independent of β_c . It then follows that $\mathcal{V}_j \rightarrow 0$ if and only if $NB \gg MC$ for BBFS channels. The transition to the condition $N \gg M$ for NBFF channels takes place when $B \sim C$, i.e. $\tau \sim B^{-1}$.

The stability condition can be interpreted as follows: NB is the number of degrees of freedom in the CSI collected at the TRA per unit time; MC is the number of degrees of freedom in the ensemble of messages per unit time; the stability condition $NB \gg MC$ says that in order to recover the input

messages, independent of the channel realization, and thus reverse the random scrambling by the channel, the former must be much larger than the latter. In light of this interpretation, the stability condition derived above appears to be sharp.

A detailed, rigorous analysis of the MIMO-TR channel modeled by a stochastic Schrödinger equation, in the parabolic approximation of scalar waves, with a random potential is given in [12].

4 Rate of information transfer

In this section we discuss the information rate for a memoryless channel which is constructed out of the time-invariant channel model analyzed in Section 3. The temporal dependence is introduced by drawing an independent realization from the Rayleigh-fading ensemble of transfer matrices after each use of the channel, i.e. after each delay spread (or two if the time for channel estimation is included). This is obviously an idealization but widely used in communications literature [31], [15]. The coherence time of the resulting ergodic channel model is then much longer than one delay spread. We assume as in standard practice that in addition to the random channel fluctuations additive-white-Gaussian-noise (AWGN) is present at each receiver, that the input signal vector is multivariate Gaussian and that the channel, the noise and the input signal are mutually independent.

For the Rayleigh fading channel prior to adding noise, each frequency component of the time reversed signal S_j in (3)

$$\begin{aligned}
& \sum_{i=1}^M \sum_{k=1}^N m_i(\tau_l) g\left(\frac{\omega - \omega_0}{B}\right) H_{jk}(\omega) H_{ik}^*(\omega) \\
= & \underbrace{\sum_{k=1}^N m_i(\tau_l) g\left(\frac{\omega - \omega_0}{B}\right) H_{jk}(\omega) H_{jk}^*(\omega)}_{N\text{-degree central } \chi^2 \text{ r.v.}} + \underbrace{\sum_{i \neq j} \sum_{k=1}^N m_i(\tau_l) g\left(\frac{\omega - \omega_0}{B}\right) H_{jk}(\omega) H_{ik}^*(\omega)}_{N(M-1) \text{ i.i.d. zero-mean r.v.s}}
\end{aligned}$$

is a sum of a central χ^2 random variable with N degrees of freedom and $N(M-1)$ i.i.d. mean-zero random variables. This is due to the assumption that different entries of the transfer matrix are mutually independent zero-mean Gaussian random variables. Therefore, for $N \gg 1$ the interference statistic is approximately Gaussian, by the Central Limit Theorem. More generally, after synthesizing all the available frequencies, the interference statistic becomes approximately Gaussian if $NB\beta_c^{-1} \gg 1$ which is always the case for the BBFS channels. In a BBFS (resp. NBFF) channel, $NB\beta_c^{-1}$ (resp. N) is the number

of independent subchannels from TRA to each receiver.

Moreover, each frequency component of S_j has the mean

$$\mathbb{E}\left[\sum_{i=1}^M \sum_{k=1}^N m_i(\tau_l) g\left(\frac{\omega - \omega_0}{B}\right) H_{jk}(\omega) H_{ik}^*(\omega)\right] = N\sigma g\left(\frac{\omega - \omega_0}{B}\right) m_j(\tau_l). \quad (7)$$

which exhibits the simple input-output relation: The ω -component of the input signal for the j -th receiver is $m_j g(\omega)$ and the received signal component is $N\sigma m_j g(\omega)$ corrupted by the noise and interference which for $N \gg 1$ is approximately Gaussian. Since the M receivers operate independently of one another, the total time-reversal broadcast channel consists of M independent subchannels in parallel each of which has the above input-output relation. Thus the total information rate is the sum of those of the M subchannels from TRA to individual receivers. And, in view of the simple input-output relation, each subchannel can be viewed as a single-input-single-output (SISO) linear filter channel corrupted by (approximately) Gaussian noise/interference for which Shannon's theorem is applicable.

According to Shannon's theorem [5] the ergodic capacity (in nats per unit time and frequency) of a SISO linear filter channel is $\ln(1 + \text{SINR})$ where **SINR**, the signal-to-interference-and-noise ratio at each receiver, is given by the harmonic sum of the **SIR**, the signal-to-interference ratio and **SNR**, the signal-to-noise ratio, i.e. $\text{SINR} = (\text{SIR}^{-1} + \text{SNR}^{-1})^{-1}$. For extension of Shannon's result to the MIMO setting, see [15], [31].

Analogous to the NBFF channels in Section 3, $\text{SIR}(\omega) = \mathcal{V}_j^{-1} \sim N/M$, independent of μ and ω . Let ν be the noise power, per unit frequency, at each receiver. Suppose the average transmission power is constrained to P and all the transmit and receive antennas are identical.

Since the value of σ would affect **SNR** (but not **SIR**) we discuss the two cases $N \geq M$ and $N < M$ separately.

Case 1: $N \geq M$. In this case, $\sigma = N^{-1}$ and in view of (7), $\text{SNR}(\omega) = \mu^2/\nu$ where $\mu = |m_j|$ can be related to the total power constraint P as $\mu^2 M \sim P/B$ since the average input power per unit frequency is

$$\sum_{k=1}^N \sum_{i=1}^M |m_i(\tau_l)|^2 |g|^2 (B^{-1}(\omega - \omega_0))^2 \mathbb{E}|H_{ik}(\omega)|^2 \sim MN\sigma\mu^2 = M\mu^2.$$

Thus $\text{SNR}(\omega) \sim P/(\nu BM)$. Therefore the total channel capacity (in nats per

unit time) is roughly given by

$$BM \ln \left[1 + \frac{1}{M} \left(\frac{1}{N} + \frac{\nu B}{P} \right)^{-1} \right]. \quad (8)$$

Now we ask the question: What is the maximal rate at which a TRA, with fixed number of elements N , fixed average total power P and fixed noise level (per frequency) ν , can transfer information if there is no limitation to the number of receivers M and the bandwidth B ?

Expression (8) can be optimized at the limit $M \gg P/(\nu B)$ to yield the optimal information rate of P/ν which is linearly proportional to the power. We see that the simplest strategy for optimizing the information rate of a given TRA under the the power and noise constraints is to enlarge the bandwidth B as much as possible. And if we can satisfy $N \gg M \gg P/(\nu B)$ then we can achieve stability as well as the optimal information rate.

Consider the thermal noise power $\nu = k_B T$ where k_B is the Boltzmann's constant and T the temperature. Then the above result implies that the energy cost per nat is $P/R \sim k_B T$ which is consistent with the classical result of minimum energy $k_B T$ requirement for transmitting one nat information at temperature T [24], [21].

Case 2. $N \leq M$. In this case, $\sigma = M^{-1}$ and (7) implies that $\text{SNR} \sim N^2 \mu^2 / (M^2 \nu)$ where μ is related to P by $\mu^2 = P/(NB)$. Hence $\text{SNR} \sim NP/(M^2 \nu B)$. With $\text{SIR} \sim N/M$ and Shannon's theorem, the channel capacity is roughly

$$BM \ln \left(1 + \frac{N}{M} \left(1 + \frac{MB\nu}{P} \right)^{-1} \right) \quad (9)$$

which achieves the optimal rate P/ν in the regime $N = M \gg P/(B\nu)$. On the other hand, for $M \ll P/(B\nu)$, the information rate becomes $BM \ln (1 + N/M) \leq BN$ which is much smaller than P/ν .

Therefore we conclude that under the power and noise constraints the condition for the optimal information rate P/ν is $N \geq M \gg P/(B\nu)$, which can be achieved by sufficiently large bandwidth, whereas the additional condition $N \gg M$, which, sufficient for the Gaussian approximation to the interference statistic, would also guarantee stability.

Before ending this section, let us compare the capacity in the conventional, non-TR MIMO channel as calculated in [15], [31], [22], [30]. Consider the non-TR single-user channel with the M transmit antennas (on the right of Fig. 1) which have no channel knowledge and the $N(\geq M)$ receive antennas (on the left of Fig. 1) as the single user which has perfect CSI. This is, of

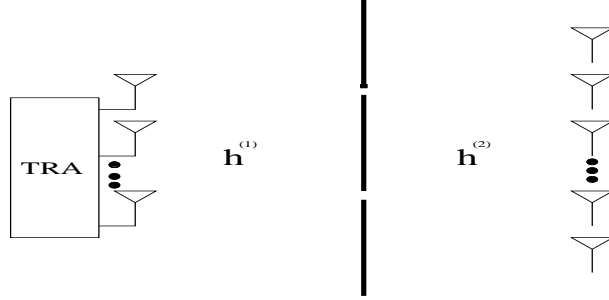


Fig. 2. Single-screen pinholes

course, the reciprocal case of the TR broadcast channel. In this case, $\text{SNR} \sim P/(MB\nu)$ and it is shown in [15] and [31] that the ergodic capacity of the single-user narrowband Rayleigh-fading channel scales like $BM \ln \text{SNR}$ at high SNR which can be recovered from (8) by imposing the additional constraint $M \leq P/(\nu B) \leq N$. And as we learn from the discussion of Case 1 above, this is *not* the regime for achieving the optimal information rate P/ν .

The same results as discussed in this section are obtained for the parabolic Markovian channel model in [12].

5 Pinhole effect

Pinholes are degenerate channels that can occur in a wide family of channels, outdoor as well as indoor, see Fig. 2 and 3. While preserving the co-channel decorrelation, pinholes have been shown to severely limit the degrees of freedom and reduce the channel capacity [3], [16], [4]. In this section, we introduce the notion of effective number of TRA elements to analyze the multi-screen pinhole effect on TR in Rayleigh fading.

Let us begin with the simplest case of single-screen pinholes as illustrated in Fig. 2. Let $\mathbf{h}^{(1)}(\omega)$ be the $N \times K$ transfer matrix from the TRA to the pinholes and $\mathbf{h}^{(2)}(\omega)$ the $K \times M$ transfer matrix from the pinhole to the M receivers at frequency ω . The combined channel can be described by $\mathbf{H}(\omega) = \mathbf{h}^{(2)}(\omega)\mathbf{h}^{(1)}(\omega) = [\sum_{k=1}^K h_{ik}^{(2)}(\omega)h_{kj}^{(1)}(\omega)]$ in which $h_{kj}^{(1)}(\omega)$ and $h_{ij}^{(2)}(\omega)$ are assumed to be independent $\mathcal{CN}(0, \sigma_1)$ and $\mathcal{CN}(0, \sigma_2)$, respectively, and $\{h_{ij}^{(1)}(\omega), h_{ij}^{(2)}(\omega)\}_{i,j,\omega}$, are jointly Gaussian processes. To prevent the average input power from being less than the average output power we set $\mathbb{E}|H_{ij}|^2 = K\sigma_1\sigma_2 = (N \vee M)^{-1}, \forall i, j$. Note that the entries of \mathbf{H} are in general *not* independent r.v.s.

As before we assume the frequency coherence structure

$$\mathbb{E}[h_{ij}^{(k)}(\omega)h_{i'j'}^{(k)*}(\omega')] \approx \sigma_k f\left(\frac{\omega - \omega'}{\beta_c}\right) \delta_{i'i'} \delta_{j'j}, \quad \forall k \quad (10)$$

where, for simplicity, f and β_c are taken to be independent of the screens. Straightforward calculations with the Gaussian rule show that the mean signal is

$$\mathbb{E}[S_j(t)] = BNK\sigma_1\sigma_2 \sum_{l=1}^W m_j(\tau_l) \mathcal{F}^{-1}[g](B(\tau_l - t))$$

and its variance is

$$\begin{aligned} V_j(t) = & \sigma_1^2 \sigma_2^2 NK \sum_{l,l'=1}^W e^{i\omega_0(\tau_l - \tau_{l'})} \int d\omega d\omega' e^{-i\omega(t - \tau_l)} e^{i\omega'(t - \tau_{l'})} g\left(\frac{\omega}{B}\right) g^*\left(\frac{\omega'}{B}\right) |f|^2\left(\frac{\omega - \omega'}{\beta_c}\right) \\ & \times \left(m_j(\tau_l) m_j^*(\tau_{l'}) + N \sum_{i=1}^M m_i(\tau_l) m_i^*(\tau_{l'}) + K |f|^2\left(\frac{\omega - \omega'}{\beta_c}\right) \sum_{i=1}^M m_i(\tau_l) m_i^*(\tau_{l'}) \right) \quad (11) \end{aligned}$$

In view of the observations following eq. (6) we have the estimate $V_j(t) \sim B^2 KN(MN + MK + 1)\sigma_1^2 \sigma_2^2 |\mu|^2$ for the NBFF channels and $V_j(t) \sim BCKN(MN + MK + 1)\sigma_1^2 \sigma_2^2 |\mu|^2$ for the BBFS channels. As in (6) the variance does not depend on the coherence bandwidth β_c . Therefore we obtain the normalized variance of the signal to the leading order ($N, K \gg 1$)

$$\mathcal{V}_j \approx \begin{cases} M(N^{-1} + K^{-1}), & \text{for the NBFF channels} \\ MCB^{-1}(N^{-1} + K^{-1}), & \text{for the BBFS channels.} \end{cases}$$

The result suggests the notion of *effective* number of TRA-elements given by $N_{\text{eff}} = NK(N + K)^{-1}$, namely the harmonic sum of N and K , so that $\mathcal{V}_j \approx MCB^{-1}N_{\text{eff}}^{-1}$ for the BBFS channels and $\mathcal{V}_j \approx MN_{\text{eff}}^{-1}$ for the NBFF channels. For $N, K \gg 1$ the number of statistically independent paths is roughly $N_{\text{eff}} \times M$.

The previous case *without* pinholes corresponds to the limiting case $K \gg N$. For a fixed K , however, the previous benefit of stability with large number of TRA elements ($N \gg 1$) disappears. The multiple antennas in TRA are essentially screened out by the pinholes and the effective number of TRA-elements becomes K .

5.1 Multi-screen pinholes

The same analysis can be applied to channels with $(n - 1)$ screens of pinholes such as illustrated in Fig. 3. Let $K_k, k = 1, \dots, n - 1$ be the number of k -th screen pinholes. Let $\mathbf{h}^{(k)}$ be the transfer matrix for the k -th stage channel whose

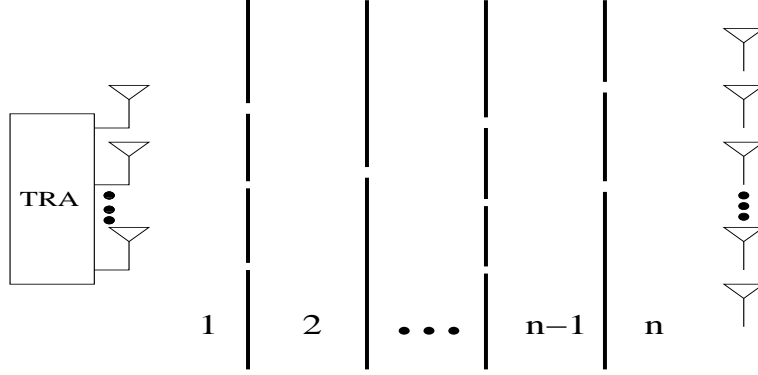


Fig. 3. Multi-screen pinholes

entries are independent $\mathcal{CN}(0, \sigma_k)$ and let the transfer matrices of different stages be mutually independent. Again, in order for the average input power to be no less than the average output power we set

$$\mathbb{E}|H_{ij}|^2 = K_1 \cdots K_{n-1} \sigma_1 \cdots \sigma_n = (N \vee M)^{-1}. \quad (12)$$

The condition of statistical stability, however, is independent of the values of $\sigma_k, k = 1, \dots, n$.

As noted previously the the normalized variance does not depend on β_c and its order of magnitude is determined solely by the same-frequency moments which will be the focus of the subsequent calculation. The calculation of the mean is straightforward: $\mathbb{E}(\mathbf{H}\mathbf{H}^\dagger \mathbf{m})_j = NK_1 \cdots K_{n-1} \sigma_1 \cdots \sigma_n m_j$. Let us analyze the second moment of entry a

$$\begin{aligned} & \mathbb{E}(\mathbf{H}\mathbf{H}^\dagger \mathbf{m})_a (\mathbf{H}\mathbf{H}^\dagger \mathbf{m})_a^* \\ &= \mathbb{E} \left\{ \sum_{\substack{i_1, \dots, i_n \\ j_2, \dots, j_{n+1}}} h_{ai_n}^{(n)} h_{i_n, i_{n-1}}^{(n-1)} \cdots h_{i_3, i_2}^{(2)} h_{i_2, i_1}^{(1)} h_{j_2, i_1}^{(1)*} h_{j_3, j_2}^{(2)*} \cdots h_{j_n, j_{n-1}}^{(n-1)*} h_{j_{n+1}, j_n}^{(n)*} m_{j_{n+1}} \right. \\ & \quad \times \left. \sum_{\substack{i'_1, \dots, i'_n \\ j'_2, \dots, j'_{n+1}}} h_{ai'_n}^{(n)*} h_{i'_n, i'_{n-1}}^{(n-1)*} \cdots h_{i'_3, i'_2}^{(2)*} h_{i'_2, i'_1}^{(1)*} h_{j'_2, i'_1}^{(1)} h_{j'_3, j'_2}^{(2)} \cdots h_{j'_n, j'_{n-1}}^{(n-1)} h_{j'_{n+1}, j'_n}^{(n)} m_{j'_{n+1}}^* \right\}. \end{aligned}$$

According to the Gaussian rule for computing moments, the above expression can be represented by 2^n diagrams of $4n$ vertexes and $2n$ edges. We distinguish two types of edges: the *arcs*, connecting (un)primed indices to (un)primed indices, and the *ladders*, connecting unprimed indices to primed indices, see Fig. 4.

When a new screen of pinholes, represented by $\mathbf{h}^{(n+1)}$, is added, the number of diagrams is doubled: one half of them contain the ladders connecting $h_{ai_{n+1}}^{(n+1)}$ to $h_{ai'_{n+1}}^{(n+1)*}$ and $h_{j_{n+2}, j_{n+1}}^{(n+1)*}$ to $h_{j'_{n+2}, j'_{n+1}}^{(n+1)}$ while the other half contain the arcs con-

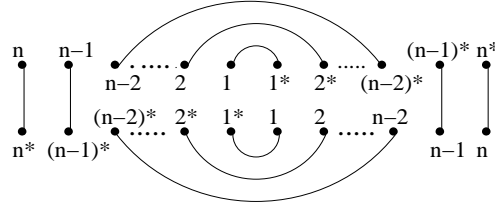


Fig. 4. Separable diagram: * means complex conjugation; the top indices are unprimed and the bottom indices are primed.

necting $h_{ai_{n+1}}^{(n+1)}$ to $h_{j_{n+2}, j_{n+1}}^{(n+1)*}$ and $h_{ai'_{n+1}}^{(n+1)*}$ to $h_{j'_{n+2}, j'_{n+1}}^{(n+1)}$. Straightforward calculation with (10) yields the following rule: A new pair of arcs add to diagrams with outermost arcs the K_n^2 (multiplicative) factor and diagrams with outermost ladders the K_n/M factor; on the other hand, a new pair of ladders add to diagrams with outermost ladders the K_n^2 factor and diagrams with outermost arcs the $K_n M$ factor.

That is, the diagrams that correspond to the highest power in K_1, K_2, \dots , have the least number of edge-type alternating. Hence for $K_1, \dots, K_{n-1} \gg 2^n \gg N$ the leading order term in the variance corresponds to the diagram with all ladders and is of order $K_1^2 \dots K_{n-1}^2 NM$ while the square of the mean corresponds to the diagram with all arcs and is of order $K_1^2 \dots K_{n-1}^2 N^2$. The stability condition thus remains the same as in the case without pinholes.

Let us consider the more interesting regime in which $N, K_1, \dots, K_{n-1} \gg 2^n$. We claim that to the leading order the normalized variance of the signal is given by $\mathcal{V}_j \approx MCB^{-1}N_{\text{eff}}^{-1}$ where the effective number of TRA-element N_{eff} is given by

$$N_{\text{eff}} = (N^{-1} + N_p^{-1})^{-1}, \quad N_p = \left(\sum_{j=1}^{n-1} K_j^{-1} \right)^{-1};$$

namely the harmonic sum of N, K_1, \dots, K_{n-1} . We sketch the proof here. The leading order terms in the variance after expectation correspond to the *separable* diagrams in which the arcs are nested and are flanked by the ladders, Fig. 4. Except for the diagram with all ladders, the separable diagrams all have the innermost arcs connecting $h_{i_2, i_1}^{(1)}$ to $h_{j_2, i_1}^{(1)*}$ and $h_{i_2', i_1'}^{(1)*}$ to $h_{j_2', i_1'}^{(1)}$, which give rise to the factors N^2 (an extra N than otherwise), and, except for the diagrams with all ladders or all arcs, the separable diagrams change the edge-type exactly once (from arc to ladder). When N is comparable to K_1, \dots, K_{n-1} , the contributions from the separable diagrams are comparable to that from the diagram of all edges.

Collecting the terms corresponding to the separable diagrams we have

$$\mu^2 NM \prod_{i=1}^n \sigma_i^2 \prod_{j=1}^{n-1} K_j \left(\prod_{k=1}^{n-1} K_k + N \sum_{i=1}^{n-1} K_1 \cdots \widehat{K}_i \cdots K_{n-1} \right)$$

where \widehat{K}_i means that K_i is absent in the product. Dividing it by $N^2 \prod_{i=1}^{n-1} K_i^2$ and accounting for the temporal aspect of transmission as in the observations following eq. (6) we obtain the claimed result.

5.2 Information rate with pinholes

The notion of the effective number of TRA elements is useful in estimating the channel capacity as well as the stability condition in the presence of pinholes since SIR is given by N_{eff}/M with $C = 2B$.

As the (spatial) subchannel from TRA to each receiver is the sum of $NK_1K_2 \cdots K_{n-1}$ paths which are not necessarily independent, the simplest way for realizing Gaussian interference statistic is to assume large degrees of freedom in frequency $B\beta_c^{-1} \gg 1$ so that each spatial subchannel gives rise to a sum of $B\beta_c^{-1}$ roughly i.i.d. r.v.s. This works only for the BBFS channels. For the NBFF channels, we assume the worst-case scenario $K_{\min} = \min[N, K-1, \dots, K_{n-1}] \gg 1$ because each subchannel can be regrouped into a sum of $NK_1K_2 \cdots K_{n-1}/K_{\min}$ terms each of which is a sum of K_{\min} i.i.d. r.v.s.

Due to the normalization (12) the input-output relation in (7) and the discussion in Section 4 (Case 1 & 2) remain valid if N is replaced by N_{eff} . In particular, the same optimal information rate P/ν is achieved in the regime $N_{\text{eff}} \wedge M \gg P/(B\nu)$.

As analyzed before, when the condition $N, K_1, \dots, K_{n-1} \gg 2^n$ is satisfied, N_{eff} is the harmonic sum of N, K_1, \dots, K_{n-1} and therefore we have the estimates: $K_{\min}/n \leq N_{\text{eff}} \leq K_{\max}/n$ where K_{\min} and K_{\max} are the minimum and maximum of N, K_1, \dots, K_{n-1} , respectively. On the other hand, when $N, K_1, \dots, K_{n-1} \ll 2^n$, diagrammatic analysis shows that N_{eff} diminishes exponentially with the number of screens, making the alternative regime $N_{\text{eff}} \leq P/(B\nu)$ much more likely and resulting in low information rate BN_{eff} (cf. Case 2, Section 4). In other words, a long chain of independently fluctuating media separated by a series of screens of *sparse* pinholes is detrimental to time reversal (and perhaps any) communication systems

6 Conclusions

We have analyzed the time reversal propagation in independent-multipath Rayleigh-fading MIMO-channels with or without pinholes. The focus of the analysis is the stability condition, the multiplexing gain and the multi-screen pinholes effect. The main results are (i) that the stability holds when $MC \ll N_{\text{eff}}B$ for the BBFS channels and $M \ll N_{\text{eff}}$ for the NBFF channels where N_{eff} is the effective number of TRA-elements, (ii) that the optimal information rate P/ν under the power and noise constraints is achieved in the regime $N_{\text{eff}} \wedge M \gg P/(B\nu)$ and (iii) that the effective number of TRA-elements is asymptotically the harmonic sum of TRA-elements and the numbers of pinholes on all $n - 1$ screens when the numbers of TRA-elements and the pinholes of each screen are greater than 2^n . The notion of the effective number of TRA elements is introduced for the first time and shown to be useful in analyzing stability and capacity in the presence of pinholes.

References

- [1] P. Blomgren, G. Papanicolaou and H. Zhao, *J. Acoust. Soc. Am.* 111(2002), 230-248.
- [2] Bruesselbach, D.C. Jones and D.A. Rockwell and R.C. Lind, *J. Opt. Soc. Am.* B 12(1995), 1434-1447.
- [3] D. Chizhik, G. J. Foschini and R.A. Valenzuela, *IEEE Electron. Lett.* 36 (2000), 1099-1100.
- [4] D. Chizhik, G. J. Foschini, M.J. Gans and R.A. Valenzuela, *IEEE Trans. Wireless Comm.*1(2)(2002), 361-368.
- [5] T.M. Cover and J.A. Thomas, *Elements of Information Theory* Wiley, New York, 1991.
- [6] A. Derode, E. Larose, M. Tanter, J. de Rosny, A. Tourin, M. Campillo and M. Fink, *J. Acoust. Soc. Am.*113 (2003), 2973.
- [7] A. Derode, A. Tourin and M. Fink, *Phys. Rev. E* 64 (2001), 036606.
- [8] A. Derode, A. Tourin and M. Fink, *Ultrasonics* 40(2002), 275-280.
- [9] A. Derode, A. Tourin, J. de Rosny, M. Tanter, S. Yon, and M. Fink, *Phys. Rev. Lett.*90(2003), 014301.
- [10] G. Edelmann, T. Akal, W. S. Hodgkiss, S. Kim, W. A. Kuperman, H. C. Song, *IEEE J. Oceanic Eng.* 27 (2002), 602-609.
- [11] A. Fannjiang, *J. Stat. Phys.*120(2005), 543-586.

- [12] A. Fannjiang, *e-print*: arxiv.org/abs/physics/0509158.
- [13] A. Fannjiang and K. Solna, *Phys. Lett. A* 352:1-2 (2005), 22-29.
- [14] M. Fink, D. Cassereau, A. Derode, C. Prada, P. Roux, M. Tanter, J.L. Thomas and F. Wu, *Rep. Progr. Phys.* 63(2000), 1933-1995.
- [15] G.J. Foschini and M.J. Gans, *Wireless Personal Comm.* 6 (1998), 311-335.
- [16] D. Gesbert, H. Bolcskei, D. Gore and A. Paulraj, in *Proc. CT10-5, IEEE Globecom 2000*, San Francisco, CA. Nov. 27-Dec. 1, 2000.
- [17] S. Kim, W. A. Kuperman, W. S. Hodgkiss, H. C. Song, G. Edelmann, and T. Akal, *J. Acoust. Soc. Am.* 114 (2003), 145-157.
- [18] A. D. Kim, P. Kyritsi, P. Blomgren and G. Papanicolaou, preprint, 2004.
- [19] A. Lagendijk and B. A. van Tiggelen, *Phys. Rep.* 270 (1996), 143-215.
- [20] G. Lerosey, J. de Rosny, A. Tourin, A. Derode, G. Montaldo, and M. Fink, *Phys. Rev. Lett.* 92(2004), 193904.
- [21] L.B. Levitin, *Phys. D.* 120 (1998), 162-167.
- [22] A.L. Moustakas, H.U. Baranger, L. Balents, A.M. Sengupta and S.H. Simon, *Science* 287 (2000), 287-290.
- [23] A. Paulraj, R. Nabar and D. Gore, *Introduction to Space-Time Wireless Communications*, Cambridge University Press, 2003.
- [24] J. R. Pierce, *IEEE Trans. Commun.* COM-26(1978), 1819-1921. Reprinted in *Quantum Theory and Measurement*, J. A. Wheeler and W. H. Zurek ed., Princeton University Press, Princeton, 1983.
- [25] D. Rouseff, D. R. Jackson, W. L. J. Fox, C. D. Jones, J. A. Ritcey and D. R. Dowling, *IEEE J. Oceanic Eng.* 26 (2001), 821-831.
- [26] K.G. Sabra, S.R. Khosla and D.R. Dowling, *J. Acoust. Soc. Am.* 111(2) (2002), 823-830.
- [27] P. Sebbah, B. Hu, A.Z. Genack, R. Pnini and B. Shapiro, *Phys. Rev. Lett.* 88 (2002), 123901.
- [28] B. Shapiro, *Phys. Rev. Lett.* 57 (1986), 21682171.
- [29] P. Sheng: *Introduction to Wave Scattering, Localization, and Mesoscopic Phenomena*, Academic Press, Boston, 1995.
- [30] S.H. Simon, A.L. Moustakas, M. Stoychev and H. Safar, *Phys. Today* 54:9 (2001), 38.
- [31] I.E. Telatar, *European Trans. Tel.* 10 (1999), 585-595.